

## A novel synthesis of tin oxide thin films by the sol-gel process for optoelectronic applications

M. Marikkannan,<sup>1</sup> V. Vishnukanthan,<sup>2</sup> A. Vijayshankar,<sup>3</sup> J. Mayandi,<sup>1,4,a</sup>  
and J. M. Pearce<sup>4,5,b</sup>

<sup>1</sup>Department of Materials Science, School of Chemistry, Madurai Kamaraj University,  
Tamilnadu, Madurai-625021, India

<sup>2</sup>Department of Physics, Centre for Materials Science and Nanotechnology, University  
of Oslo, P.O. Box 1126 Blindern, N-0318 Oslo, Norway

<sup>3</sup>Department of Physics and Technology, University of Bergen, Allegaten 55, N-5007, Bergen,  
Norway

<sup>4</sup>Department of Materials Science & Engineering, Michigan Technological University, USA

<sup>5</sup>Department of Electrical & Computer Engineering, Michigan Technological University, USA

(Received 12 January 2015; accepted 5 February 2015; published online 13 February 2015)

A novel and simple chemical method based on sol-gel processing was proposed to deposit metastable orthorhombic tin oxide (SnO<sub>x</sub>) thin films on glass substrates at room temperature. The resultant samples are labeled according to the solvents used: ethanol (SnO-EtOH), isopropanol (SnO-IPA) and methanol (SnO-MeOH). The variations in the structural, morphological and optical properties of the thin films deposited using different solvents were characterized by X-ray diffraction, atomic force microscopy, Raman spectroscopy, Fourier transform infrared (FTIR) spectroscopy, UV-vis spectroscopy and photoluminescence (PL) analysis. The XRD patterns confirm that all the films, irrespective of the solvents used for preparation, were polycrystalline in nature and contained a mixed phases of tin (II) oxide and tin (IV) oxide in a metastable orthorhombic crystal structure. FTIR spectra confirmed the presence of Sn=O and Sn-O in all of the samples. PL spectra showed a violet emission band centered at 380 nm (3.25 eV) for all of the solvents. The UV-vis spectra indicated a maximum absorption band shown at 332 nm and the highest average transmittance around 97% was observed for the SnO-IPA and SnO-MeOH thin film samples. The AFM results show variations in the grain size with solvent. The structural and optical properties of the SnO thin films indicate that this method of fabricating tin oxide is promising and that future work is warranted to analyze the electrical properties of the films in order to determine the viability of these films for various transparent conducting oxide applications. © 2015 Author(s). All article content, except where otherwise noted, is licensed under a Creative Commons Attribution 3.0 Unported License. [<http://dx.doi.org/10.1063/1.4909542>]

### I. INTRODUCTION

Transparent conducting oxides (TCOs) materials are known for the rare combination of electrical conductivity and optical transparency.<sup>1-3</sup> These materials are generally prepared using thin film deposition methods and are widely used in optoelectronic devices such as gas sensors, batteries, photo-catalysts, flat-panel displays, photoelectron chemical devices, and solar photovoltaic (PV) cells. A transparent p-n type junction is needed for a range of future transparent devices in order to function effectively. Unfortunately, the stable p-type materials available at present still lack optimal electronic properties such as high hole mobility and controllable hole density, and hence show low conductivity compared to equivalent n-type counterpart materials.<sup>4-8</sup> Thus, further exploration is

<sup>a</sup>Contact author: [jeyanthinath@yahoo.co.in](mailto:jeyanthinath@yahoo.co.in)

<sup>b</sup>Contact author: [pearce@mtu.edu](mailto:pearce@mtu.edu)



needed into high conductivity p-type materials. In recent years, tin (II) oxide has attracted significant attention due to its native p-type conductivity and stability in maintaining both structure and electronic properties for many years.<sup>9</sup> As tin oxides possess a high density of delocalized Sn 5s and Sn 5p states in the valence band and conduction band, respectively, it is one of the most promising materials for transparent applications involving future optoelectronic devices.<sup>10</sup>

Tin oxides (SnOx) are generally available in two oxidation states, divalent (tin (II) oxide - SnO) and tetravalent (tin (IV) oxide - SnO<sub>2</sub>) and are termed as p-type and n-type semiconductors, respectively.<sup>11,12</sup> SnO<sub>2</sub> thin films can be prepared by pulsed laser deposition, ultrasound-assisted and microwave-assisted methods, thermal, electron beam evaporation, sputtering, vapor-liquid-solid synthesis, hydrothermal deposition, spray pyrolysis and sol-gel methods.<sup>13-16</sup> Among the various techniques to produce tin oxide, the sol-gel method is one of the most promising because it is relatively simple process that enables straight-forward control of thin film properties. Kim *et al.* reported that films prepared using sol gel methods were suitable for device applications.<sup>17</sup> However, the preparation of solution for the fabrication of SnO is critical as the divalent nature of this material can be easily degraded into a tetravalent state due to oxidation during preparation.<sup>18</sup>

Under normal conditions, tin (IV) oxide exists in the rutile phase (R-SnO<sub>2</sub>), and has been extensively studied by many researchers.<sup>19,20</sup> However, under high pressure and temperature fabrication, the orthorhombic SnO<sub>2</sub> (O-SnO<sub>2</sub>) is expected. To the best of our knowledge, no reports on the fabrication of orthorhombic-SnO (O-SnO) using the low temperature sol gel method can be found in literature.

In this study O-SnO and O-SnO<sub>2</sub> thin films were prepared with the Sol-Gel Spin Coating method (SGSC) using three different solvents ethanol, isopropanol and methanol and labeled SnO-EtOH, SnO-IPA, and SnO-MeOH, respectively. Structural and optical properties of the SnO<sub>x</sub> thin films prepared using this array of solvents were characterized using X-ray diffraction (XRD), atomic force microscopy (AFM), UV-vis spectroscopy, Fourier transform infrared spectroscopy (FTIR), Raman analysis and photoluminescence (PL). The results were presented and the effects of the solvent on crystal structure, surface morphology and optical properties of SnOx thin films was discussed and conclusions were drawn.

## II. EXPERIMENTAL

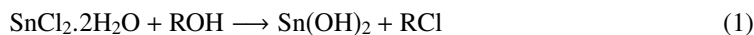
### A. Materials

The materials used in this investigation were SnCl<sub>2</sub>·2H<sub>2</sub>O (Purified from Merck), ethanol (99.9% Channshu Yangyuan), isopropanol (Merck) and methanol (Sigma Aldrich).

### B. Methods

The tin oxide films were prepared using SnCl<sub>2</sub>·2H<sub>2</sub>O and alcohol as the Sn and O precursors, respectively. Initially, sol was prepared by dissolving 0.5 mole of SnCl<sub>2</sub>·2H<sub>2</sub>O in one of the three solvents: ethanol, isopropanol and methanol. The prepared solution was magnetically stirred for 5 hours in a closed container and aged for 24 hours at room temperature to increase the viscosity. Before spin coating, the glass substrates were pre-cleaned with acetone, isopropanol and distilled water. The as-prepared sol was spin coated on a glass substrate maintained at 1200 rpm for 30 sec. After spin coating, glass substrates were then heat treated at 100°C for 10 min. to remove the residual organic solvents. The films were deposited with ethanol, isopropanol and methanol solvents. The films synthesis was found to be highly reproducible for all of the solvents.

The following chemical reactions occur during the fabrication of tin oxide thin films:



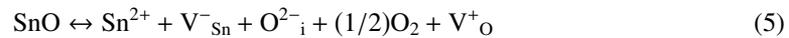
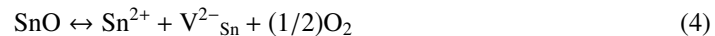
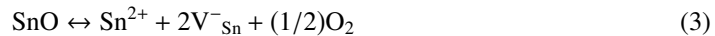
The structural properties of the films were analyzed by XRD using Cu K $\alpha$  radiation (Bruker D8). The surface morphology parameters of the films were evaluated with AFM. The optical absorption and transmittance of the samples were determined from UV-vis spectroscopy (absorption and

transmittance - Shimadzu-2450) at room temperature, FTIR and Raman analysis (Lab Ram HR 800). The PL spectra of the as-prepared thin films were recorded using a spectrofluorophotometer (Shimadzu RF-5000) and a laser with excitation wavelength of 325 nm was used as the source.

### III. RESULTS AND DISCUSSION

#### A. Crystal structure and surface morphology

The XRD peaks of the SnO-EtOH, SnO-IPA, and SnO-MeOH samples are shown in Figure 1. The diffraction peak centered at  $2\theta = 31.59^\circ$  was noted for the SnO-EtOH samples and corresponds to an orthorhombic (O) structure of SnO (JCPDS data card No: 77-2296). The SnO-IPA and SnO-MeOH samples reveal two different diffraction peaks centered at  $2\theta = 33.3^\circ$  and  $45.29^\circ$ , which corresponds to the (022) and (024) planes of O-SnO<sub>2</sub> (JCPDS date card No: 78-1063) and O-SnO, respectively. The SnO-MeOH sample further display a small and less intense peak at  $57.5^\circ$ , which corresponds to the (310) reflection of the O-SnO structure. From this initial XRD analysis, it is clear that all of the three diffraction peaks displayed in Figure 1 do not match tetragonal R-SnO<sub>2</sub> diffraction peaks. The XRD spectra shows that the SnO-EtOH film was oriented along the O-SnO (020) plane and the SnO-IPA and SnO-MeOH films had mixed phases of O-SnO and O-SnO<sub>2</sub> however isopropanol predominantly produced O-SnO<sub>2</sub> thin films. It is speculated that both the preparation conditions and oxidation performance of the different solvents were responsible for the degree of stabilization of O-SnO and O-SnO<sub>2</sub> phases. Moreover, the preferred orientation of the films also changed with the different solvents. Oxygen concentration has been established as an important parameter for controlling SnO<sub>x</sub> film formation.<sup>12</sup> In this study all the experiments were carried out in a closed container where evaporation of the solvent was negligible during the reaction and oxidation is limited by the reaction rate of different alcohols, as equal molar volumes of the oxygen precursors were taken. The formation of SnO films thus occurs in an oxygen deficient condition. The possible SnO formation stoichiometric reactions are:<sup>21</sup>



In addition to the reaction rate, the super saturation of the surface reaction minimization and thermo-dynamical equilibrium also control the formation of SnO films. This effect enhances the stoichiometry of the SnO<sub>x</sub> thin films. Degree of stabilization of O-SnO<sub>2</sub> and/ or O-SnO is attributed to the different reaction rates of the precursors. The grain sizes of the films were calculated from the

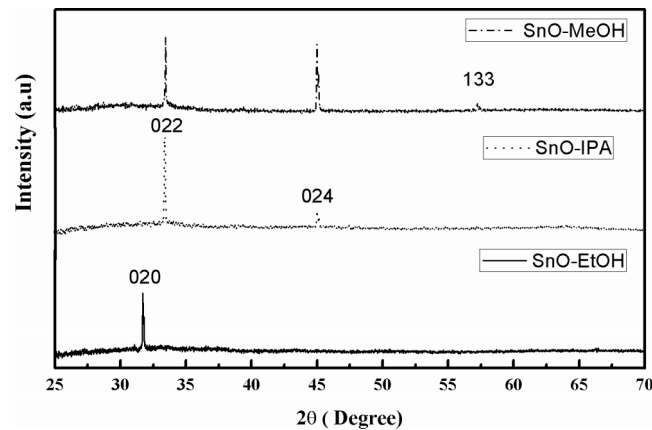


FIG. 1. XRD patterns of SnO thin films prepared with ethanol (SnO-EtOH), isopropanol (SnO-IPA), and methanol (SnO-MeOH).

TABLE I. The structural data for the SnO film samples.

Sample	Preferred Orientation	d Spacing (Å)	Lattice constant (Å)	Micro strain	Dislocation Density $\times 10^{-6} \text{ (nm)}^{-2}$	Grain Size (nm)
SnO-EtOH	020	2.8299	5.659	0.0105	1.3513	74
SnO-IPA	022	2.6884	5.408	0.0178	1.6129	62
SnO-MeOH	022	2.6837	5.398	0.0161	1.0638	94

scherrer formula:

$$D = K\lambda/\beta_{hkl}\cos\theta \quad (6)$$

Where  $D$  is the grain size in nm,  $K$  is the shape factor (0.9), and  $\lambda$  is the wavelength of Cu  $K\alpha$  radiation (0.154 nm).<sup>22</sup> The grain sizes of SnO-EtOH, SnO-IPA and SnO-MeOH films were found to be 74 nm, 62 nm, and 94 nm, respectively. The calculated d-spacing value of the samples were also in good agreement with the JCPDS values. However, these values need to be supported with the other relevant techniques described below. The preferred orientation, d spacing, lattice constant, micro strain, dislocation density and grain size were summarized for all three types of samples in Table I.

Figure 2 shows the AFM surface morphology of the SnO thin films. It should be noted that the z-axis scale in Figure 2 is not the same for all films, to make the surface morphology more clear to the observer. The surface morphological parameters are represented by the root mean square (RMS) roughness 0.49, 1.76 and 0.691 nm for SnO-EtOH, SnO-IPA and SnO-MeOH respectively. It is clear from Figure 2 that all the samples have an even surface. The least surface roughness (0.49 nm) was attained for the SnO-EtOH films (Fig. 2), although these films may also be the thinnest as there are several pinholes in the sample, which is common for excessively thin spin-coated films. Well-defined grains were observed in films prepared with the isopropanol solvent with a highly oriented nature (Fig. 2). The coalescence of the grains was observed for all the films. The samples synthesized using isopropanol and methanol demonstrate uniform coating without pinholes.

## B. Spectroscopy characterization

Figure 3 shows the Raman spectra of the SnO<sub>x</sub> thin films prepared with different solvents. All the samples demonstrate Raman modes centered at 597 and 811 cm<sup>-1</sup>. These observed modes do not match with characteristic modes of tetragonal SnO (211 cm<sup>-1</sup>A<sub>1g</sub>) and SnO<sub>2</sub> (630 cm<sup>-1</sup>A<sub>1g</sub>) reported elsewhere.<sup>23-25</sup> In agreement with XRD observations, the Raman spectrum related

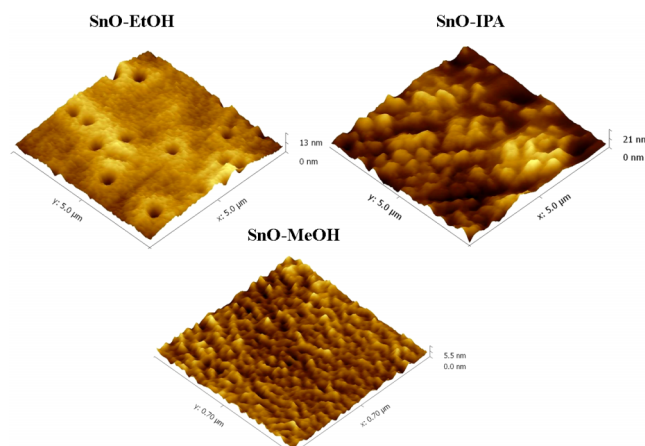


FIG. 2. AFM images showing the morphology of SnO-EtOH, SnO-IPA and SnO-MeOH thin films.

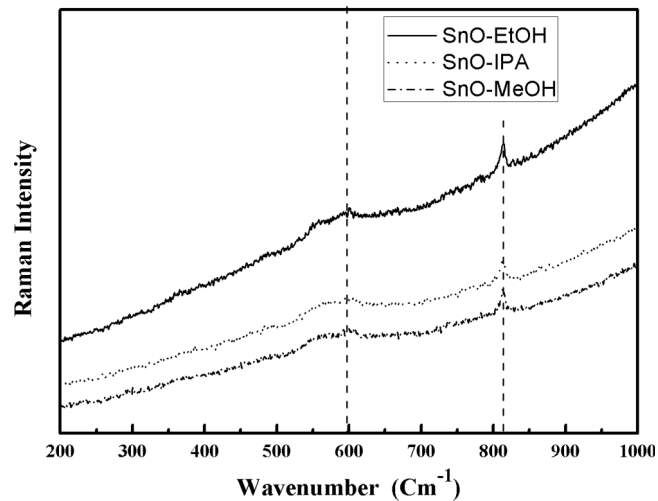


FIG. 3. Raman spectra of SnO-EtOH, SnO-IPA and SnO-MeOH thin films.

to tetragonal structures is not found in any of these samples. At this time no theoretical data are available in the literature to assign the observed Raman shifts and is left for future work.

The FTIR transmittance spectra of the SnO<sub>x</sub> thin films are shown in Figure 4. A peak at 773 cm<sup>-1</sup> was observed for the SnO-EtOH and SnO-MeOH films, which corresponds to a O-Sn-O bond.<sup>26</sup> The peak attained at around 960 cm<sup>-1</sup> for SnO-EtOH and SnO-MeOH thin films and 903 cm<sup>-1</sup> for SnO-IPA films correspond to Sn-O vibration.<sup>27</sup> These corresponding peaks confirm the formation of SnO<sub>x</sub> films. Peaks observed in SnO-IPA films at around 1500 cm<sup>-1</sup> were weak and were attributed to the OH in-plane deformation mode.<sup>28</sup> The strong band at 2358 cm<sup>-1</sup> was absorbed for SnO-EtOH and SnO-IPA films that correspond to an antisymmetric CO<sub>2</sub> stretching vibration. Additional impurity modes were also observed in the FTIR spectra in all samples, which were caused during chemical synthesis and require post-treatments to eliminate.

The UV-vis. absorption spectra for spin coated SnO<sub>x</sub> thin films were shown in Figure 5(A). UV absorption peaks were observed at 323, 332 and 331 nm for SnO-EtOH, SnO-IPA, and SnO-MeOH samples, respectively. These spectra indicate that the SnO-IPA samples show the highest absorption capacity. Figure 5(B) shows the transmission spectra of the tin oxide thin films. All the samples show an optical average transmittance between 89 and 97% in the visible region, which is in a

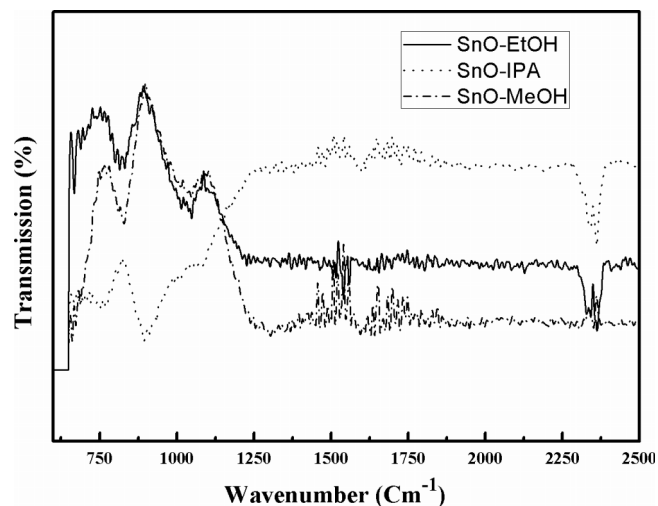


FIG. 4. FTIR spectra of SnO thin films prepared by various solvents.

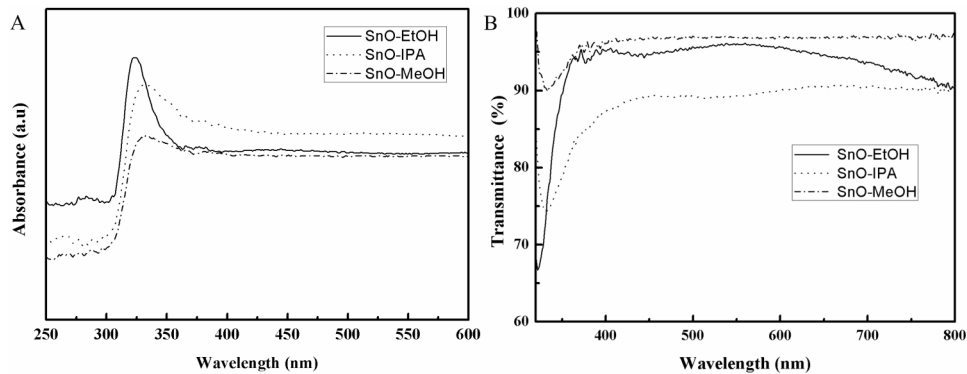


FIG. 5. (A) UV-visible absorption spectra for SnO thin films (B) Optical transmittance spectra for SnO thin films.

good range for many optoelectronics application. The average transmittance in the visible region for the SnO-EtOH, SnO-IPA and SnO-MeOH samples were estimated to be 95%, 89%, and 97%, respectively. Out of the three samples, the thin film prepared with methanol, shows the highest value of average transmission. This can be explained as the larger grain size observed for methanol films (94 nm), which leads to the reduction of scattering effects and enhances the transmittance. The optical band gap can also be determined from Tauc plots using transmission spectra. For the direct allowed transition, the optical band gap energy of the tin oxide films is determined using:<sup>29</sup>

$$\alpha h\nu = A(h\nu - E_g)^{1/2}. \quad (7)$$

Where  $\alpha$  is the absorption coefficient,  $A$  is a proportional constant,  $h$  is Planck's constant and  $\nu$  is the frequency of vibration so  $h\nu$  is the photon energy and  $E_g$  is the optical band gap of the material. Typical Tauc plots of  $h\nu$  vs  $(\alpha h\nu)^{1/2}$  were made for all the samples. The resultant to optical band gaps ( $E_g$ ) were found to be 3.3 eV for the SnO-EtOH samples and 2.9 eV for both the SnO-IPA and SnO-MeOH samples. These band gap values were in good agreement with the previously reported values of SnO thin films. Allen *et al.* reported optical band gaps of the SnO thin films ranging from 2.5 to 3.3 eV.<sup>30</sup> Direct band gap materials are more efficient than indirect band gap materials for many different applications,<sup>18</sup> in particular for device applications like solar photovoltaic cells. Direct band gap materials usually allow the minimum energy transition from the valence band to the conduction band without changing the wave vector ( $k$ ). But an indirect band gap material requires the wave vector to be changed with phonons for electron transitions to occur. Hence, the preliminary data obtained here indicates that SnO thin films prepared in this work may be suitable for the device applications as the results obtained closely match predicted direct band gap values.

The room temperature PL spectra of the tin oxide thin films using ethanol, isopropanol and methanol solvents were shown in Figure 6. The PL emission bands were observed at around 363, 381 and 413nm, respectively. There is also a minor intensity shoulder band centered at 413 nm for all samples. The violet emission band centered at around 381 nm for all the samples corresponds to 3.25 eV, or the band-to-band transition in the materials. The observed corresponding energy value also closely matches the values estimated from the Tauc plots. The shoulder peak at 413 nm closely matches with the luminescence centers formed by the tin inertial or dangling bonds reported in the literature.<sup>31</sup>

This work proposes a novel method for the preparation of metastable orthorhombic SnO thin films with the simple sol gel method: films prepared employing low temperature process and were investigated and the resultant structural and optical properties of the films were systematically analyzed to determine the effects of the solvent. As the nature of this process is inherently low-cost: this work may be a platform to prepare p-type SnO thin films using a simple and reproducible method for future research. Future work is needed to characterize the electrical properties and explore other deposition variables to optimize the films for optoelectronic device applications. Furthermore, the film thicknesses and the effects of changing annealing temperatures will need to be investigated in detail to further optimize film properties for specific applications.

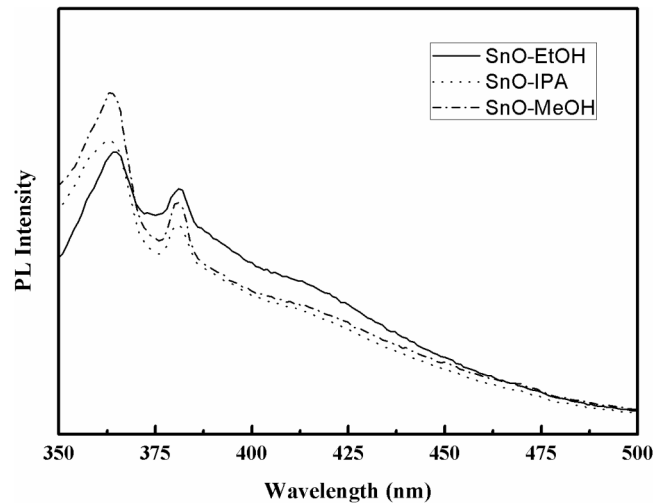


FIG. 6. Photoluminescence spectra of SnO thin films with the excitation wavelength of 325 nm at room temperature.

#### IV. CONCLUSIONS

Metastable orthorhombic SnO<sub>x</sub> thin films were successfully prepared on glass substrates at room temperature using a novel yet simple chemical method. The structural results indicated that the films were preferentially oriented along the (020) and (022) directions for all the samples. However, using isopropanol and methanol as the precursor resulted in the stabilization of both (022) O-SnO<sub>2</sub> and (024) O-SnO and was attributed to the different reaction rates of the precursors. Structural results confirmed the presence of the nanosized grains in the SnO thin films. The vibrational modes of the films also coincide with the reported values with the presence of Sn=O and Sn-O bonds. The highest absorption (332 nm) and highest average transmittance (97%) was obtained for isopropanol and methanol based films, respectively. These results indicate that this method of fabricating tin oxide is promising and future work is needed to analyze the electrical properties of the films in order to determine the viability of these films for various TCO applications.

#### ACKNOWLEDGMENTS

The authors are thankful to the **DST-SERB/F/1829/2012-2013** for partial support of this research. The authors would like to thank M. Mohan Raj and P. Jayabal for FTIR and UV, PL measurements. JM thanks the UGC for providing support through the RAMAN fellowship 2014-2015 to visit Michigan Technological University, USA.

- <sup>1</sup> K. Zhang, F. Zhu, C. H. A. Huan, and A.T.S. Wee, *J.Appl.Phys* **86**, 2 (1999).
- <sup>2</sup> X. Liu, D. Zhang, Y. Zhang, and X. Dai, *J.Appl.Phys* **107**, 64309 (2010).
- <sup>3</sup> J. Huang, X. Xu, C. Gu, S. Yao, Y. Sun, and J. Liu, *CrystEnggComm* **14**, 3233 (2012).
- <sup>4</sup> T. garden, *Nature* **389** (1997).
- <sup>5</sup> E. Fortunato, P. Barquinha, and R. Martins, *Adv. Mater* **24**, 2945 (2012).
- <sup>6</sup> H. Hosono, Y. Ogo, H. Yanagi, and T. Kamiya, *Electrochemical and Solid-State Letters* **14**, H13 (2011).
- <sup>7</sup> Y. Ogo, H. Hiramoto, K. Nomura, H. Yanagi, T. Kamiya, M. Hirano, and H. Hosono, *Appl. Phys. Lett* **93**, 032113 (2008).
- <sup>8</sup> E. Fortunato and R. Martins, *Phys. Status Solidi RRL* **5**, 336 (2011).
- <sup>9</sup> W. Guo, Fu.L. Zhang, Y. Zhang, L.Y. Liang, Z.M. Liu, H.T. Cao, and XQ Pan, *Appl. Phys. Lett* **96**, 042113 (2010).
- <sup>10</sup> B.D. Granato, J.A. Caraveo-Frescas, H.N. Alshareef, and U. Schwingenschlogl, *Appl. Phys. Lett* **102**, 212105 (2013).
- <sup>11</sup> J.M. Xu, L. Li, S. Wang, H.L. Ding, Y. X. Zhang, and G. H. Li, *CrystEnggComm* **15**, 3296 (2013).
- <sup>12</sup> X. Liu, D. Zhang, Y. Zhang, and X. Dai, *J.Appl.Phys* **107**, 064309 (2010).
- <sup>13</sup> X. Xu, M. Ge, K. Stahl, and J.Z. Jiang, *Chemical Physics Letters* **482**, 287 (2009).
- <sup>14</sup> H. Yabuta, N. Kaji, R. Hayashi, H. Kumomi, K. Nomura, T. Kamiya, M. Hirano, and H. Hosono, *Appl. Phys.Lett.* **97**, 072111 (2010).
- <sup>15</sup> C. Thanachayanont, V. Yordsri, and C. Boothroyd, *Materials Letters* **65**, 2610 (2011).
- <sup>16</sup> K. Okamura, B. Nasr, R. A. Brand, and H. Hahn, *J. Mater. Chem* **22**, 4607 (2012).
- <sup>17</sup> M-G. Kim, M. G. Kanatzidis, A. Facchetti, and T. J.Marks, *Nature Materials* **10** (2011).
- <sup>18</sup> K. Sakasui, Y. Oaki, H. Uchiyama, E. Hosono, H. Zhou, and H. Imai, *Nanoscale* **2**, 2424 (2010).

- <sup>19</sup> P. Sangeetha, V. Sasirekha, and V. Ramakrishnan, *J. Raman Spectroscopy* **42**, 1634 (2011).
- <sup>20</sup> J.M. Xu, L. Li, S. Wang, H.L. Ding, Y.X. Zhang, and G.H. Li, *CrystEnggComm* **15**, 3296 (2013).
- <sup>21</sup> E. Fortunato, R. Barros, P. Barquinha, V. Figueiredo, S.H. Ko Park, C-S. Hwang, and R. Martins, *Appl.Phys.Lett* **97**, 052105 (2010).
- <sup>22</sup> V.D. Mote, Y. Purushotham, and BN. Dole, *Journal of Theoretical and Applied Physics* **6.6** (2012).
- <sup>23</sup> X. Wang, F.X. Zhang, I. Loa, K. Syassen, M. Hanfland, and Y.L. Mathi, *Phys.Stat.Sol (b)* 3168 (2004).
- <sup>24</sup> J. Geurts, S. Rau, W. Richter, and F.J. Schmitte, *Thin Solid Films* **121**, 217 (1984).
- <sup>25</sup> Y.Q. Guo, R.Q. Tan, X. Li, J.H. Zhao, Z. L. Luo, C. Gao, and W.J. Song, *CrystEngcomm* **13**, 5677 (2011).
- <sup>26</sup> A.S. Aji and Y. Darma, *AIP Conference Proceedings* **93**, 55410 (2013).
- <sup>27</sup> S.K. Pillai, L. M. Sikhwivhilu, and Thembela K. Hillie, *Synthesis Chemistry and Physics* **12**, 010 (2012).
- <sup>28</sup> J. Zawadzki, 147 (1989).
- <sup>29</sup> SK. F. Ahmed, S. Khan, P.K. Ghosh, M.K. Mitra, and K. K. Chattopadhyay, *J Sol-Gel Sci Technn* **39**, 241 (2006).
- <sup>30</sup> J. P. Allen, D. O. Scanlon, S. C. Parker, and G. W. Watson, *Phys.Chem.Chem.C* **115**, 19916 (2011).
- <sup>31</sup> W. Bing and X. Ping, *Chinese Physics B* **18**, 1 (2010).